



THE UNIVERSITY *of* EDINBURGH

## Edinburgh Research Explorer

### Nanoband array electrode as a platform for high sensitivity enzyme-based glucose biosensing

**Citation for published version:**

Falk, M, Sultana, R, Swann, MJ, Freeman, NJ & Mount, A 2016, 'Nanoband array electrode as a platform for high sensitivity enzyme-based glucose biosensing', *Bioelectrochemistry*, vol. 112, pp. 100-105.  
<https://doi.org/10.1016/j.bioelechem.2016.04.002>

**Digital Object Identifier (DOI):**

[10.1016/j.bioelechem.2016.04.002](https://doi.org/10.1016/j.bioelechem.2016.04.002)

**Link:**

[Link to publication record in Edinburgh Research Explorer](#)

**Document Version:**

Version created as part of publication process; publisher's layout; not normally made publicly available

**Published In:**

Bioelectrochemistry

**General rights**

Copyright for the publications made accessible via the Edinburgh Research Explorer is retained by the author(s) and / or other copyright owners and it is a condition of accessing these publications that users recognise and abide by the legal requirements associated with these rights.

**Take down policy**

The University of Edinburgh has made every reasonable effort to ensure that Edinburgh Research Explorer content complies with UK legislation. If you believe that the public display of this file breaches copyright please contact [openaccess@ed.ac.uk](mailto:openaccess@ed.ac.uk) providing details, and we will remove access to the work immediately and investigate your claim.





Contents lists available at ScienceDirect

Bioelectrochemistry

journal homepage: [www.elsevier.com/locate/bioelechem](http://www.elsevier.com/locate/bioelechem)

## Nanoband array electrode as a platform for high sensitivity enzyme-based glucose biosensing

Magnus Falk<sup>a,\*</sup>, Reshma Sultana<sup>a</sup>, Marcus J. Swann<sup>a</sup>, Andrew R. Mount<sup>b</sup>, Neville J. Freeman<sup>a</sup>

<sup>a</sup> NanoFlex Limited, iTac, Daresbury Laboratory, Sci-Tech Daresbury, Keckwick Lane, Daresbury WA4 4AD, United Kingdom

<sup>b</sup> EaStCHEM, School of Chemistry, The University of Edinburgh, Joseph Black Building, King's Buildings, Edinburgh, Scotland EH9 3JJ, United Kingdom

### ARTICLE INFO

#### Article history:

Received 5 October 2015

Received in revised form 29 March 2016

Accepted 8 April 2016

Available online xxxx

#### Keywords:

Nanoband array electrode

Biosensor

Glucose oxidase

Glucose

### ABSTRACT

We describe a novel glucose biosensor based on a nanoband array electrode design, manufactured using standard semiconductor processing techniques, and bio-modified with glucose oxidase immobilized at the nanoband electrode surface. The nanoband array architecture allows for efficient diffusion of glucose and oxygen to the electrode, resulting in a thousand-fold improvement in sensitivity and wide linear range compared to a conventional electrode. The electrode constitutes a robust and manufacturable sensing platform.

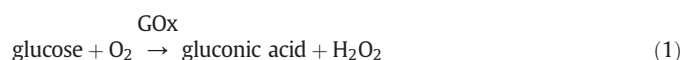
© 2016 Elsevier B.V. All rights reserved.

### 1. Introduction

Enzyme-based electrochemical biosensors are used for a multitude of applications; they employ a wide variety of oxidoreductases, and are found in many analytical instruments used in environmental, food, pharmaceutical and clinical laboratories [1]. The stand-out, most successful application is electrochemical biosensors for glucose sensing; these now help millions of diabetic people manage their condition, and many new biosensor designs are reported yearly in the literature [2,3]. Some type 1 diabetics find it difficult to manage hypoglycaemic events, which can lead to the need for emergency medical intervention. One means to reduce the need for such intervention is to employ Continuous Glucose Monitoring (CGM) devices which are implanted under the skin, where they reside for typically a week. CGM has proven very useful for understanding and managing individual patient therapeutic regimes. However, a number of challenges are faced in this field including poor device accuracy, narrow linear range and the short lifetime of implanted devices [4]. Apart from invasive sensors, wearable electrochemical sensors have received considerable recent interest and could potentially be employed for CGM, operating in tears, sweat or saliva [5].

Many glucose biosensors use additional electroactive mediators to operate. Due to the possible toxicity of the mediators [6], their use in implantable devices is however problematic, e.g. in CGM devices. Another

common way to produce a glucose sensor, also employed in the majority of the CGM devices currently on the market [4], is to use a so-called first generation glucose biosensor design, where GOx turns over glucose in the presence of its natural co-substrate oxygen, producing hydrogen peroxide [2]. Hydrogen peroxide is then electrochemically oxidised at a Pt electrode by applying an anodic potential:



One drawback with such a biosensor design is that the concentration of dissolved oxygen is typically much lower than that of the glucose, meaning that the response of the device is determined by the availability of oxygen [3]. Oxygen and glucose concentrations need to be controlled with diffusion membranes, which necessarily also reduces the glucose concentration at the electrode surface and generates mass transfer limitations [7,8].

By employing different nanomaterials in the design of biosensors, considerable improvements in sensitivity, selectivity, and accuracy can be achieved [9,10]. Different nanomaterials such as nanoparticles, nanofibres, nanotubes and nanocomposites have been used to modify macro-scale electrodes. Many different strategies have been developed to immobilise enzymes on these nanostructured macro-electrodes, which have resulted in enhanced redox currents. This has been achieved by stabilising surface interactions with the adsorbed enzymes and

\* Corresponding author.

E-mail address: [magnus.falk@nanoflex.com](mailto:magnus.falk@nanoflex.com) (M. Falk).

presenting a high surface-to-volume ratio to enable a high enzyme load [11].

Instead of employing nanomaterials-modified macro-scale electrodes in the biosensor design, another approach is to use nanoelectrodes or nanoelectrode arrays [6,12,13]. The electrochemical properties of nanoelectrodes differ significantly from those of macro-scale electrodes, and are characterised by enhanced and often steady-state (time independent) diffusion. This enhanced mass transport provides several benefits, including increased signal-to-noise ratio and high sensitivity. This has already been shown to provide high sensitivity for biorecognition reactions [13,14]. Thus, an important potential application of nanoelectrodes is in bioanalytical measurement systems, e.g. for healthcare applications, where the improved sensitivity can expand the range of target analyte molecules to include those which are currently considered to be at impracticably low levels in situ, as well as to improve the overall performance of the biodevice.

In the present paper we employ a nanoband array electrode, fabricated using processes standard to the semiconductor industry with very high reproducibility, to produce a high-sensitivity enzymatic glucose sensor operating by immobilising the glucose oxidase (GOx) enzyme on the electrode surface. This utilizes the common first-generation approach as employed in many commercial CGM devices to illustrate the potential benefit a nanoband array could have in biosensing [4]. The nanoband array electrode demonstrates a thousand-fold improvement compared to a similarly designed macro electrode, attributed to the particular properties of the nanoscale electrode architecture.

## 2. Experimental

### 2.1. Materials

All chemicals used were of analytical grade and were purchased from Sigma Aldrich, UK. Glucose oxidase from *Aspergillus niger*,  $149.8 \text{ U mg}^{-1}$ , was used for the enzyme modification. All solutions were prepared using deionised water with a measured ionic resistivity of  $18.2 \text{ M}\Omega \text{ cm}$ . An air-saturated  $10 \text{ mmol dm}^{-3}$  phosphate buffered saline (PBS), pH 7.4, containing  $0.0027 \text{ mol dm}^{-3}$  potassium chloride and  $0.137 \text{ mol dm}^{-3}$  sodium chloride was used throughout all experiments. Glucose stock solutions ( $0.1 \text{ mol dm}^{-3}$ ) were prepared with PBS and were allowed to mutarotate overnight before use. A Pt Microsquare Nanoband Edge Electrode (MNEE, Fig. 1 c) (CAVIARE™ Nanoband Array, Platinum 303D, NanoFlex Limited, UK), discussed in more detail in Section 3.1, or a  $100 \mu\text{m}$  diameter Pt disc electrode were bi-modified and used as working electrodes.

The fabrication processes used to obtain MNEE architectures are standard to the semiconductor industry, employing thin film techniques and lithography. As a result the device yields are extremely high (>98%) with excellent reproducibility from device to device

(typical relative standard deviations < 1%). The approach is also compatible for use with flexible substrates using processing techniques that are currently widely used for the mass production of commercial disposable electrochemical test strip devices at comparable manufacturing costs.

### 2.2. Electrode modification

Prior to use, the MNEE was cleaned electrochemically by cycling the potential between  $-0.35$  and  $1.9 \text{ V}$  (vs. SCE) at a scan rate of  $100 \text{ mV s}^{-1}$  for 10 cycles in  $0.05 \text{ mol dm}^{-3} \text{ H}_2\text{SO}_4$ . The MNEE was then incubated in conc.  $\text{H}_2\text{SO}_4$  for 3 min followed by  $50\% \text{ H}_2\text{SO}_4$  for another 3 min and thereafter rinsed copiously with water. To create the glucose sensor, the Pt MNEE was first modified with 6-Mercaptohexylamine thiol (MHA). Apart from gold, thiols are also known to form well-defined monolayers on other metals, such as Pt [21,22]. Thiol modification was performed by incubating the MNEE for 20 h in  $50 \mu\text{mol dm}^{-3}$  of MHA dissolved in ethanol. The electrode was thereafter rinsed with ethanol followed by water. After thiol modification, the electrode was incubated for 45 min in  $20 \mu\text{L}$   $8\%$  glutaraldehyde solution (dissolved in water). Afterwards, the electrode was carefully rinsed with buffer and  $20 \mu\text{L}$  of  $40 \text{ mg ml}^{-1}$  GOx (dissolved in buffer) was pipetted over the MNEE and left covered to prevent evaporation for 2 h. The electrodes were finally rinsed with buffer and ready for use. The Pt disc electrode was prepared in a similar.

### 2.3. Electrochemical measurements

All electrochemical experiments were carried out in a Faraday cage using a DY2322 digital bipotentiostat (Digi-IVY, USA). The electrochemical cell consisted of a three-electrode system using a Pt MNEE or Pt disc electrode as working electrode, platinum wire counter electrode and a saturated calomel electrode (SCE) as reference. All electrochemical experiments were carried out at room temperature. Prior to addition of analyte, the working electrode was pre-conditioned by cycling the potential 10 times between  $0.2$  and  $0.9 \text{ V}$ , where hydrogen peroxide will be oxidised at the platinum surface. For glucose measurements, the measurement solution was stirred at  $600 \text{ rpm}$  using a magnetic stirrer bar to prevent build-up of hydrogen peroxide. Calibration curves of enzyme modified electrodes towards glucose were constructed from chronoamperometry measurements at  $+0.7 \text{ V}$  vs. SCE, averaging the current at  $60 \text{ s}$  over 3 repeats, whilst stirring the solution.

## 3. Results and discussion

### 3.1. Glucose sensing at MNEE vs. disc electrode

We have previously demonstrated a Platinum (Pt) Microsquare Nanoband Edge Electrode (MNEE) structure which was designed and produced by utilising standard semiconductor processes and

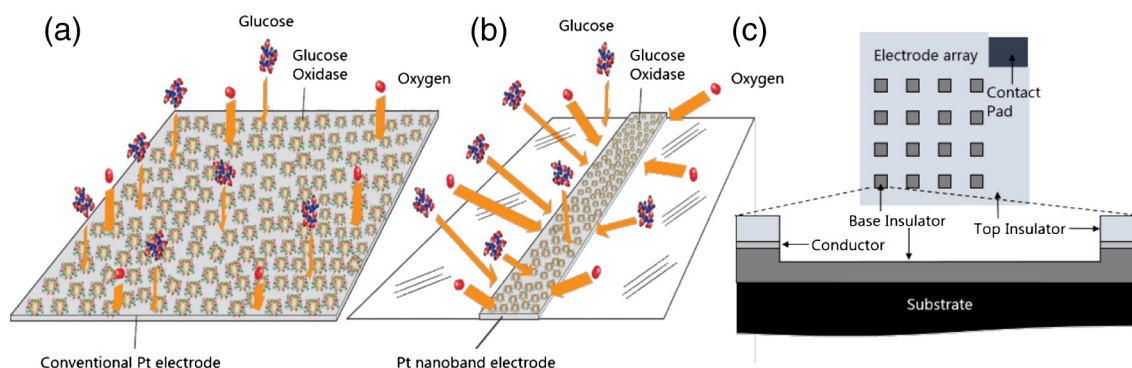


**Fig. 1.** Diffusion field at a conventional and nanoband electrode. Illustration of the planar diffusion field of a conventional planar electrode (a) compared with the local diffusion field in close proximity to a single nanoband within an aperture (b). (c) Schematic of the MNEE, not to scale.

procedures, to give an electrode array with reproducible nanoelectrode performance and relatively large currents, and which was shown to have a high sensitivity for several common redox species [14,15]. The MNEE consists of  $30 \times 30 \mu\text{m}$  edge length square apertures with a  $120 \mu\text{m}$  pitch, producing  $42 \times 42$  square elements. Within the recessed walls of each aperture there is a  $50 \text{ nm}$  thick layer of exposed Pt, which forms a nanoband electrode (Fig. 1c). The MNEE formed has a total electrode area of  $0.0106 \text{ mm}^2$  and provides a very stable and robust platform for sensing. The architecture is described in more detail elsewhere, where the mass transport-limited response is shown to be reproducible, sensitive and steady-state (at short times, before diffusion layer overlap from neighbouring array apertures occurs) [16,17]. In the context of glucose sensing, the enhanced sensitivity obtainable with a nanoband array electrode is of benefit, as this utilizes the enhanced hemispherical diffusion to the electrode [16].

Specifically, the detection of glucose at a MNEE compared with a macro-scale electrode is illustrated in Fig. 1. For planar devices the current is time dependent and proportional to the square root of the substrate diffusion coefficient, consistent with the expected linear diffusion regime for glucose or oxygen, whereas for the MNEE it is directly proportional to the diffusion coefficient, consistent with expected nanoband edge electrode response [16]. Thus whilst physiological oxygen concentrations are substantially lower than those of glucose, the fourfold greater diffusion coefficient of the former and the diffusion regime associated with the nanoband electrode significantly extend the concentration range over which glucose can be measured before the so-called oxygen deficit becomes apparent [18]. This reduces the nanoelectrode sensitivity to limitations of oxygen concentration by reducing mass transfer-based limitations and would be further enhanced for implantable devices, where tissue formation around the implant would impede the diffusion of glucose to a greater extent than that of oxygen [19,20].

### 3.2. MNEE as a glucose sensor

To characterise the performance of the MNEE as a sensor, the detection of hydrogen peroxide both on bare and enzyme-modified electrodes was first investigated. Fig. 2a shows typical cyclic voltammograms of a bare MNEE to increasing amounts of hydrogen peroxide in phosphate buffered saline (PBS) at a scan rate of  $0.1 \text{ V s}^{-1}$ . A large catalytic response towards oxidation of hydrogen peroxide was observed, even at low concentrations, compared with the very low background current in buffer (solid line in Fig. 2a, barely visible).

The electrodes were investigated over a wide concentration range of hydrogen peroxide using cyclic voltammetry, and the current response at  $+0.7 \text{ V}$  vs. SCE, consistent with oxidation potentials commonly used

in biosensors [2], is plotted as a function of concentration in Fig. 2b. The electrodes display a wide linear response and high sensitivity, with a current response of  $2.44 \mu\text{A} (\text{mmol dm}^{-3})^{-1}$   $\text{H}_2\text{O}_2$  (equal to  $23 \text{ mA} (\text{mmol dm}^{-3})^{-1} \text{ cm}^{-2}$ ), which was reduced by almost 30% when the MNEE was modified with thiol and enzyme. A reduction in the current of the bio-modified electrode is expected, as there is no glucose in the solution to enable enzyme catalysed glucose oxidation and the thiol-enzyme surface layer will inhibit transport of peroxide to the surface. Due to the low current of the blank and high current from the peroxide oxidation, very sensitive measurements are possible. This indicates that the Pt MNEE would be very suitable as a highly sensitive first generation type glucose biosensor.

To investigate the sensitivity of the MNEE towards glucose, sequential additions of glucose were performed. The results of an enzyme-modified MNEE are shown in Fig. 3. The CVs show a clear peaked shaped response when glucose is added to the solution which in accordance with Fig. 2 is characteristic of hydrogen peroxide oxidation, produced due to the catalytic oxidation of glucose. No response was observed when no glucose was present (solid curve in Fig. 3a), when a bare MNEE was used or when the solution was deoxygenated by bubbling with nitrogen (data not shown). This shows that the enzyme is catalytically active on the surface in the presence of glucose.

In addition to cyclic voltammetry the electrodes were also investigated using chronoamperometry in order to create a well-defined calibration curve. Chronoamperometry was recorded for increasing concentrations of glucose and the measurements were performed by stepping the potential from  $+0.2 \text{ V}$  to  $+0.7 \text{ V}$  vs. SCE. The potential was held for  $60 \text{ s}$  and three repeats were performed for each calibration point, averaging the current at  $60 \text{ s}$ . The results of the calibration experiments for enzyme-modified MNEE are shown in Fig. 3b (a typical chronoamperometric response curve is shown in SI Fig. 1). To ensure no build-up of hydrogen peroxide at the electrode surface in the presence of glucose (as shown in SI Fig. 2), the solution was stirred. In an actual device, the build-up of hydrogen peroxide could be reduced by immobilisation of an outer layer of catalase if it would be an issue, which would actively oxidize excess hydrogen peroxide [3]. If operating in the presence of very low glucose concentrations or operating continuously, this is not likely to be an issue.

Based on the data displayed in Fig. 3b, the MNEE biosensor exhibited a linear range between  $0$  and  $10 \text{ mmol dm}^{-3}$  glucose and a current response of  $27.9 \text{ nA} (\text{mmol dm}^{-3})^{-1}$  glucose (equal to  $263 \mu\text{A} (\text{mmol dm}^{-3})^{-1} \text{ cm}^{-2}$ ). The current response is ca 60 times lower for glucose compared to that observed for the same concentration of added hydrogen peroxide (see Fig. 2). This is expected, as comparing measurements of peroxide in bulk solution with peroxide measurements resulting from localised turnover of glucose, we expect significant differences in the concentrations at the electrode. In the bulk,

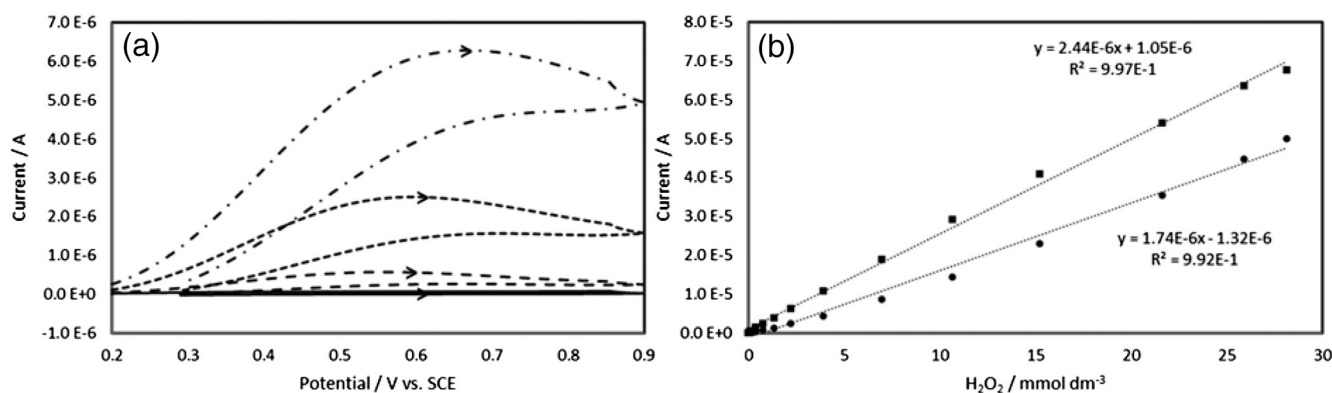


**Fig. 2.** Response to  $\text{H}_2\text{O}_2$  at a MNEE. (a) Cyclic voltammograms of a bare Pt MNEE in PBS, pH 7.4, containing  $0 \text{ mmol dm}^{-3}$  (solid line),  $0.1 \text{ mmol dm}^{-3}$  (dashed line),  $0.8 \text{ mmol dm}^{-3}$  (dotted line) and  $2.2 \text{ mmol dm}^{-3}$  (dash-dotted line)  $\text{H}_2\text{O}_2$ , recorded at a scan rate of  $0.1 \text{ V s}^{-1}$ . (b) Current of a bare (squares) and MHA-GOx-modified (circles) MNEE at increasing concentration of  $\text{H}_2\text{O}_2$ , taken from cyclic voltammograms at  $+0.7 \text{ V}$  vs. Saturated Calomel Electrode (SCE).



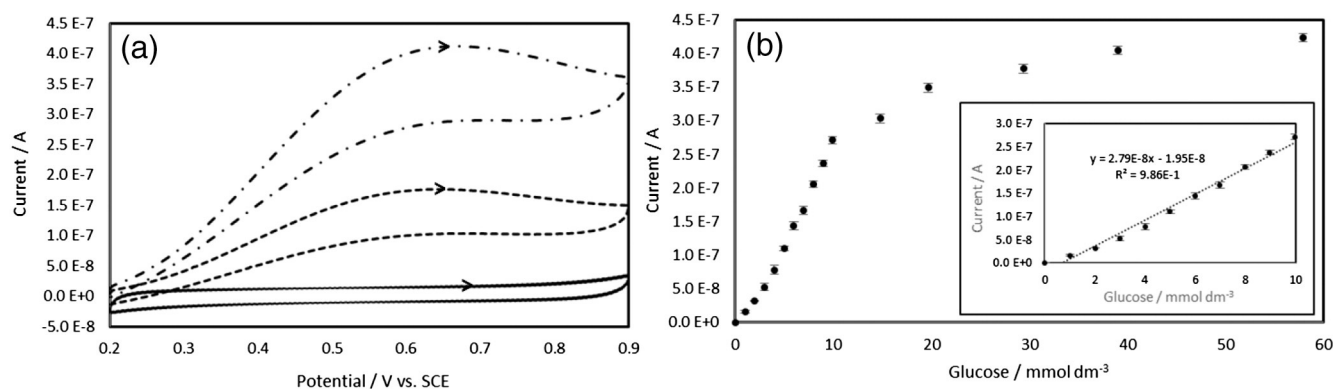


**Fig. 3.** Response to glucose at a MNEE. (a) Cyclic voltammograms of a MHA-GOx-modified Pt MNEE in 10 mmol dm<sup>-3</sup> PBS, pH 7.4, containing 0 mmol dm<sup>-3</sup> (solid line), 5 mmol dm<sup>-3</sup> (dotted line) and 10 mmol dm<sup>-3</sup> (dash-dotted line) glucose, recorded at a scan rate of 0.1 V s<sup>-1</sup>. (b) Calibration curve of enzyme modified MNEE towards glucose, constructed from chronoamperometry measurements at +0.7 V vs. SCE. Inset: Calibration curve over 0–10 mmol dm<sup>-3</sup> glucose showing the linear fit to determine the sensitivity of the electrode from the fitted slope.

concentrations of peroxide are broadly homogeneous and the electrode response will be a function of the peroxide concentration which in turn will determine the rate at which peroxide molecules reach the electrode surface. In the case of peroxide generated locally, as a consequence of glucose turnover, a localised peroxide concentration develops which results in rapid loss of peroxide to the bulk solution whose peroxide concentration tends towards zero. In the case of a stirred solution this process is enhanced, ‘sweeping’ the peroxide from the locality of the electrode. As a result, the limiting currents in the presence of glucose are significantly lower than the case of bulk peroxide measurements. However, despite the lower current response towards glucose compared with hydrogen peroxide, very sensitive measurements were possible due to the very low background signal, with the average current of the blank being roughly 0.3 nA ( $\pm 24$  pA). A Limit Of Detection (LOD) for the sensor was calculated as 2.6  $\mu\text{mol dm}^{-3}$  glucose from the data given in the calibration curve in Fig. 3b using the definition given by Commission Regulation (EC) No 333/2007: [21]

$$\text{LOD} = \frac{3 \times \text{SD}_B}{S_{CC}} \quad (3)$$

where  $\text{SD}_B$  is the standard deviation of the blank and  $S_{CC}$  is the slope of the linear fit obtained from the calibration curve.

For an oxidase-based sensor employing electrochemical oxidation of hydrogen peroxide as a detection method as described herein, a number of different compounds electroactive at the electrode potential used to oxidize hydrogen peroxide can affect the sensor response, in particular ascorbic acid. This is problematic for a sensor operating invasively (and to a lesser extent for non-invasive sensing, depending on the biofluid and presence of interferents), and a wide variety of approaches have been developed to improve the selectivity, such as permselective membranes which work via size exclusion and/or electrostatic repulsion [22]. Similar approaches could be adopted for a MNEE. The simple approach of drop-casting a Nafion membrane, a commonly used negatively charged polymer, was shown to all but eliminate the response to ascorbic acid (SI Fig. 3). Naturally, this approach would need optimization along with the enzyme deposition for an actual invasive device, with an extensive investigation of the effect different possible interferents as well as operation in the actual intended media, however this is beyond the scope of this paper.

### 3.3. Comparison with a Pt disc electrode as a glucose sensor

To illustrate the benefits the use of the MNEE brings, the performance of the enzyme-modified MNEE was compared directly with a conventional micro electrode having a similar overall electrode area. Thus a 100  $\mu\text{m}$  diameter Pt disc electrode (geometrical area of

0.0079 mm<sup>2</sup>, vs. 0.0106 mm<sup>2</sup> of exposed Pt for the MNEE), constructed as described previously [15], was modified with thiol and enzyme in the same way as the MNEE (2.2, electrode modification). The Pt disc electrode was then characterised in the same way as the MNEE, with the results shown in Fig. 4 (cf. Figs. 2a and 3b). The response towards hydrogen peroxide is shown in Fig. 4a, exhibiting 2 orders of magnitude lower current than the MNEE. Similar behaviour is observed for glucose, where the lower current leads to a much lower sensitivity towards glucose, as shown by the calibration curve in Fig. 4b, with a current response of 41.9 pA (mmol dm<sup>-3</sup>)<sup>-1</sup> glucose, roughly three orders of magnitude lower than the MNEE (cf. Fig. 3b), whilst the blank currents in buffer (no glucose present) are more than doubled for the Pt disc electrode. Based on the calibration data, a LOD of 3.5 mmol dm<sup>-3</sup> glucose was obtained for the Pt disc electrode.

By employing a MNEE instead of a similar sized (electrode area) Pt disc electrode, an improvement of three orders of magnitude in the sensitivity was achieved. No difference in the stability of the enzyme modified MNEE compared with the Pt disc electrode was observed. The wide linear range and low LOD obtained when using the enzyme-modified MNEE illustrates the large benefits achieved by employing a MNEE in the biosensor design. The increased response of the MNEE can be attributed to the enhanced mass transport to a nanoband electrode combined with the cumulative effect of an array of electrodes. This enables the high diffusional rate and high signal-to-noise ratio of nanoelectrode measurements to be combined with the high total current available with arrays, although at extended times there is an increasing overlap of the growing hemispherical diffusion layers of the individual apertures.

GOx based electrochemical glucose sensors have been extensively studied in the literature on a wide range of different support materials, such as nanoparticles, nanofibres, nanotubes and nanocomposites. The resulting material usually demonstrates high stability and reactivity, primarily attributed to the high surface area of the catalysts. A direct comparison of the performance between different approaches is often not straight forward, due to the varying measurement conditions such as rotation, oxygen concentration, use of a flow cell and measurement protocol. Typical performance shown in some of the recently reported papers display a similar linear sensing range as shown herein and a LOD of 0.5–50  $\mu\text{mol dm}^{-3}$ , with typical sensitivities of 0.5–80  $\mu\text{A (mmol dm}^{-3})^{-1} \text{ cm}^{-2}$  (cf. 263  $\mu\text{A (mmol dm}^{-3})^{-1} \text{ cm}^{-2}$  for the MNEE above) [23–29]. Indeed, the performance of the MNEE (LOD < 3  $\mu\text{mol dm}^{-3}$ ), produced using robust and reproducible silicon semiconductor fabrication techniques, is comparable to nanoparticle- or nanotube-mediated or mediatorless enzymatic glucose biosensors. Instead of relying on a high surface area to achieve a high sensitivity, the MNEE instead has a very low surface area but takes advantage of the increased mass transport due to having a nanoband

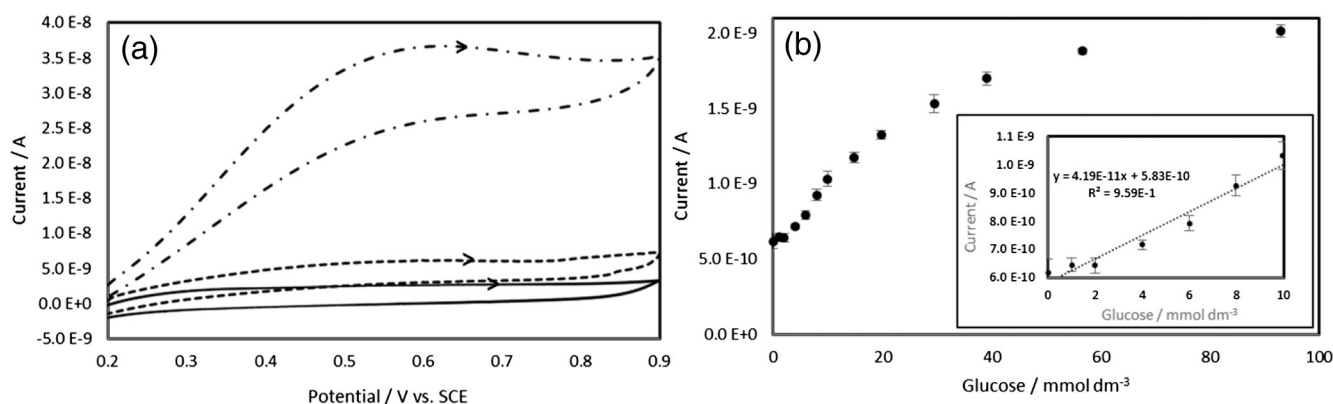


**Fig. 4.** Response to  $\text{H}_2\text{O}_2$  and glucose at a conventional electrode. (a) Cyclic voltammograms of a MHA-GOx-modified Pt disc electrode in PBS, pH 7.4, containing 0  $\text{mmol dm}^{-3}$  (solid line), 0.1  $\text{mmol dm}^{-3}$  (dotted line) and 1  $\text{mmol dm}^{-3}$  (dash-dotted line)  $\text{H}_2\text{O}_2$ , recorded at a scan rate of  $0.1 \text{ V s}^{-1}$ . (b) Calibration curve of enzyme modified Pt disc electrode towards glucose, constructed from chronoamperometry measurements at  $+0.7 \text{ V}$  vs. SCE. Inset: Calibration curve over 0–10  $\text{mmol dm}^{-3}$  glucose showing the linear fit to determine the sensitivity of the electrode from the fitted slope.

to achieve the same. The use of a MNEE thus provides a nanoparticle free alternative to more commonly nano-modified macro-scaled glucose biosensors, using materials well established in commercial devices.

The benefits shown here for a glucose biosensor would also be expected to be shown for MNEEs employed in the design of other biosensor systems. In the context of CGM, device accuracy, limited linear range and limited lifetime are ongoing challenges. Based on the data presented herein, the use of a MNEE would be expected to provide significant benefits. The efficient mass transfer and consequently wide linear range would be expected to reduce the need for membranes currently required to favour oxygen over glucose diffusion to the electrode surface [8]. The higher sensitivity exhibited by the MNEE provides the potential to reduce electrode size or increase the number of individually addressable sensors allowing for sensor redundancy with associated potential improvements in accuracy, reliability and lifetime. The high sensitivity of the sensor would also be of great importance if applied for non-invasive sensing, where the glucose is present at much lower concentrations compared to those in blood.

#### 4. Conclusions

The results reported here suggest that a significant benefit can be obtained in a common glucose sensor design by using a nanoband array electrode instead of a conventional electrode, with an improvement of three orders of magnitude achieved in the herein investigated system. This illustrates an important potential application of MNEEs in bioanalytical measurement systems, providing a robust and manufacturable sensing platform and where the improved sensitivity could expand the range of target analyte molecules to include those which are currently considered to be at impracticably low levels or inaccessible due to mass transport issues.

#### Acknowledgements

The authors wish to thank the Science and Technology Facilities Council (STFC) for their support during this research. MF acknowledges the financial support from the European Union's Seventh Framework Programme for Research, Technological Development and Demonstration under grant agreement no. 607793.

#### Appendix A. Supplementary data

Supplementary information to this article can be found online at <http://dx.doi.org/10.1016/j.bioelechem.2016.04.002>.

#### References

- [1] C.R. Ispas, G. Crivat, S. Andreescu, Review: recent developments in enzyme-based biosensors for biomedical analysis, *Anal. Lett.* 45 (2012) 168–186.
- [2] J. Wang, Electrochemical glucose biosensors, *Chem. Rev.* 108 (2007) 814–825.
- [3] A. Heller, B. Feldman, Electrochemical glucose sensors and their applications in diabetes management, *Chem. Rev.* 108 (2008) 2482–2505.
- [4] D.D. Cunningham, J.A. Stenken, *In Vivo Glucose Sensing*, Chemical Analysis, John Wiley & Sons, Hoboken, New Jersey, 2010 450.
- [5] A.J. Bandodkar, J. Wang, Non-invasive wearable electrochemical sensors: a review, *Trends Biotechnol.* 32 (2014) 363–371.
- [6] J.I. Yeh, H. Shi, Nanoelectrodes for biological measurements, *Wiley Interdisciplinary Reviews: Nanomedicine and Nanobiotechnology*, 2 2010, pp. 176–188.
- [7] S. Vaddiraju, I. Tomazos, D.J. Burgess, F.C. Jain, F. Papadimitrakopoulos, Emerging synergy between nanotechnology and implantable biosensors: a review, *Biosensors & Bioelectronics* 25 (2010) 1553–1565.
- [8] S. Vaddiraju, A. Legassey, Y. Wang, L. Qiang, D.J. Burgess, F. Jain, F. Papadimitrakopoulos, Design and fabrication of a high-performance electrochemical glucose sensor, *Journal of Diabetes Science and Technology* 5 (2011) 1044–1051.
- [9] X. Zhang, Q. Guo, D. Cui, Recent advances in nanotechnology applied to biosensors, *Sensors* 9 (2009) 1033–1053.
- [10] M. Holzinger, A. Le Goff, S. Cosnier, Nanomaterials for biosensing applications: a review, *Frontiers in Chemistry*, 2, 2014.
- [11] G. Fei, G.-H. Ma, P. Wang, Z.-G. Su, Enzyme immobilization, biocatalyst featured with nanoscale structure, *Encyclopedia of Industrial Biotechnology*, 3 2010, pp. 2086–2094.
- [12] R.G. Compton, G.G. Wildgoose, N.V. Rees, I. Streeter, R. Baron, Design, fabrication, characterisation and application of nanoelectrode arrays, *Chem. Phys. Lett.* 459 (2008) 1–17.
- [13] J.T. Cox, B. Zhang, Nanoelectrodes: recent advances and new directions, *Annu. Rev. Anal. Chem.* 5 (2012) 253–272.
- [14] R. Sultana, N. Reza, N.J. Kay, I. Schmueser, A.J. Walton, J.G. Terry, A.R. Mount, N.J. Freeman, Practical implications of using nanoelectrodes for bioanalytical measurements, *Electrochim. Acta* 126 (2014) 98–103.
- [15] N.J. Freeman, R. Sultana, N. Reza, H. Woodvine, J.G. Terry, A.J. Walton, C.L. Brady, I. Schmueser, A.R. Mount, Comparison of the performance of an array of nanoband electrodes with a macro electrode with similar overall area, *Phys. Chem. Chem. Phys.* 15 (2013) 8112–8118.
- [16] I. Schmueser, A.J. Walton, J.G. Terry, H.L. Woodvine, N.J. Freeman, A.R. Mount, A systematic study of the influence of nanoelectrode dimensions on electrode performance and the implications for electroanalysis and sensing, *Faraday Discuss.* 164 (2013) 295–314.
- [17] J.G. Terry, Schmu, x, I. ser, I. Underwood, D.K. Corrigan, N.J. Freeman, A.S. Bunting, A.R. Mount, A.J. Walton, Nanoscale electrode arrays produced with microscale lithographic techniques for use in biomedical sensing applications, *Nanobiotechnology*, IET, 7 (2013) 125–134.
- [18] W.D. Stein, Channels, Carriers, and Pumps: An Introduction to Membrane Transport, Academic Press Inc., San Diego, 1990.
- [19] A.A. Sharkawy, B. Klitzman, G.A. Truskey, W.M. Reichert, Engineering the tissue which encapsulates subcutaneous implants. I. Diffusion properties, *J. Biomed. Mater. Res.* 37 (1997) 401–412.
- [20] Z.C. Chiu, M.Y. Chen, D.J. Lee, C.H. Wang, J.Y. Lai, Oxygen diffusion in active layer of aerobic granule with step change in surrounding oxygen levels, *Water Res.* 41 (2007) 884–892.
- [21] COMMISSION Regulation (EC), Official Journal of the European Union, No 333/2007 (2007) 29–38.
- [22] S.P. Nichols, A. Koh, W.L. Storm, J.H. Shin, M.H. Schoenfisch, Biocompatible materials for continuous glucose monitoring devices, *Chem. Rev.* 113 (2013) 2528–2549.

- [23] S. Zhang, N. Wang, H. Yu, Y. Niu, C. Sun, Covalent attachment of glucose oxidase to an Au electrode modified with gold nanoparticles for use as glucose biosensor, *Bioelectrochemistry* 67 (2005) 15–22.
- [24] H. du Toit, M. Di Lorenzo, Glucose oxidase directly immobilized onto highly porous gold electrodes for sensing and fuel cell applications, *Electrochim. Acta* 138 (2014) 86–92.
- [25] X. Guo, B. Liang, J. Jian, Y. Zhang, X. Ye, Glucose biosensor based on a platinum electrode modified with rhodium nanoparticles and with glucose oxidase immobilized on gold nanoparticles, *Microchim. Acta* 181 (2014) 519–525.
- [26] D. Xiang, L. Yin, J. Ma, E. Guo, Q. Li, Z. Li, K. Liu, Amperometric hydrogen peroxide and glucose biosensor based on NiFe<sub>2</sub>/ordered mesoporous carbon nanocomposites, *Analyst* 140 (2015) 644–653.
- [27] J. Ren, W. Shi, K. Li, Z. Ma, Ultrasensitive platinum nanocubes enhanced amperometric glucose biosensor based on chitosan and nafion film, *Sensors Actuators B Chem.* 163 (2012) 115–120.
- [28] K. Zhao, S. Zhuang, Z. Chang, H. Songm, L. Dai, P. He, Y. Fang, Amperometric glucose biosensor based on platinum nanoparticles combined aligned carbon nanotubes electrode, *Electroanalysis* 19 (2007) 1069–1074.
- [29] H. Wu, J. Wang, X. Kang, C. Wang, D. Wang, J. Liu, I.A. Aksay, Y. Lin, Glucose biosensor based on immobilization of glucose oxidase in platinum nanoparticles/graphene/chitosan nanocomposite film, *Talanta* 80 (2009) 403–406.